

Generation of cumulative jets during underwater explosion of copper wires in the “X-pinch” configuration

D. Shafer, G. Toker, V. Tz. Gurovich, and Ya. E. Krasik
Physics Department, Technion, Haifa 32000, Israel

(Received 19 August 2013; accepted 11 November 2013; published online 22 November 2013)

The results of experiments with underwater electrical explosion of 0.1 mm diameter copper wires in X-pinch configuration are presented. A pulsed generator producing a ~ 30 kA-amplitude current with a ~ 65 ns rise time was used for the explosion of the wires. Shadowgraph and shearing interferometry techniques were applied for optical diagnostics. Evidence of fast-moving copper jets, originating from the location of the intersection of the exploding wires, is reported. Simultaneous measurement of the expansion of the wires, shock waves, and copper jets showed that the dynamics of the jets strongly resemble the classic problem of a collision of two planes, producing two consecutive cumulative jets. © 2013 AIP Publishing LLC.
[\[http://dx.doi.org/10.1063/1.4833553\]](http://dx.doi.org/10.1063/1.4833553)

I. INTRODUCTION

The research of electrical explosions of X-pinch configuration of wires in vacuum is attracting much attention due to the interesting physical phenomena involved in the formation of an extremely hot (>1 keV) and dense ($\sim 10^{27}$ m $^{-3}$) plasma spot at the location of the intersection of the wires, and the application of that plasma spot as a source of intense soft (≤ 10 keV) x-ray radiation, with a typical size of several microns and time duration $\leq 10^{-9}$ s.¹⁻⁵ The process of wire explosion is accompanied by the ablation of the wire material, and its ionization and compression toward the axis by the global gradient force $j \times B$ of the magnetic field,⁶ where B is the self-magnetic field of the discharge current with current density j . This force is at its maximum at the location of the plasma spot, and decreases outside the spot, along the angle bisectors in the triangle formed by the wires. This configuration of the magnetic field causes the ablated plasma to collapse onto the axis of the angle bisector, forming jet-like structures as described by Zakharov *et al.*⁷ These two oppositely aligned jets are ejected in the directions where the wires cross at acute angles.

Unlike wire explosions in vacuum, underwater electrical wire explosion⁸ (UEWE) is characterized by the confinement of the exploding wire by the surrounding water, preventing the fast radial expansion of the wire (radial expansion velocity $V_w \sim 10^3$ m/s in water versus $\sim 10^5$ m/s in vacuum). In addition, the process of parasitic plasma surface discharge, typical for wire explosions in vacuum, does not take place in UEWE due to the high ($\sim 3 \times 10^7$ V/m) threshold of the electric breakdown field in water, thus, keeping a large density discharge current flowing through the wire. As a result, a much larger energy density deposition (up to several hundreds of eV/atom) is achieved.

This paper presents the experimental results of underwater electrical explosion of wires in the X-pinch configuration. The dynamics of the resulting jets in water is found to be quite different from that in vacuum, because of the low compressibility of water. In vacuum, the effect of the generation of cumulative jets is quite weak, as described in the review by Sokolov.⁹

II. EXPERIMENTAL SETUP

The X-pinch was made of two crossed copper (Cu) wires ($\sim 58^\circ$ between the wires), each with a diameter of 0.1 mm and length of 40 mm. The wires were stretched between the cathode and anode electrodes, and immersed in water in a stainless-steel chamber having quartz windows for optical observation. The wires were exploded by a current pulse with an amplitude of $I \leq 30$ kA ($j \leq 3 \times 10^{12}$ A/m 2) and rise time of ~ 65 ns, produced by a high-current generator.⁸ The current, $I(t)$ and voltage, $\varphi(t)$ waveforms were measured using a self-integrated Rogowski coil and capacitive voltage divider, respectively (see Fig. 1).

The length and diameter of the wires were chosen such that the resulting time-dependent resistance of the exploding wires most closely matched the impedance of the generator. This allows the deposition of almost all of the stored energy (~ 300 J) into the exploding wires during the first $\tau \sim 150$ ns, resulting in an energy density deposition of $\omega_w \leq 60$ MJ/kg. Here, the energy density deposition was calculated as $\omega_w = m_w^{-1} \int_0^\tau I(t)\varphi_r(t)dt$, where m_w is the mass of the copper wire, $\varphi_r(t) = \varphi(t) - L(dI/dt)$ is the resistive component of the voltage, and L is the inductance of the load and the anode and cathode holders between the location of the voltage divider and grounded electrode.

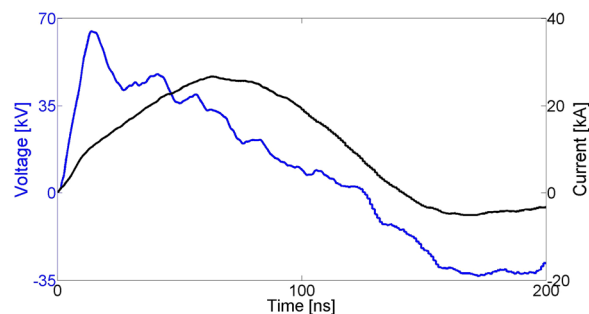


FIG. 1. Typical waveforms of the discharge voltage and current.

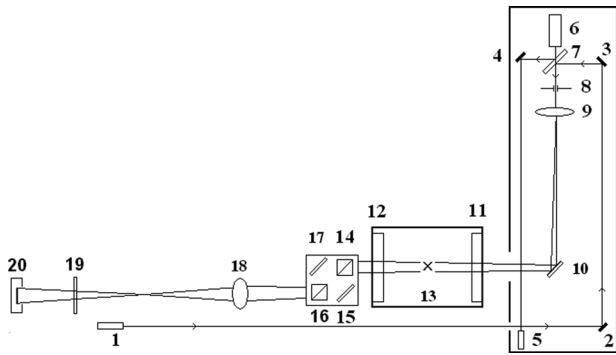


FIG. 2. Optical scheme of shearing interferometry of underwater explosion of X-pinch wires. 1: CW laser; 2, 3, 4, and 10: aluminized mirrors; 5: pulsed laser detector; 6: pulsed laser; 7: beam-splitting plate; 8: diaphragm; 9: lens; 11,12: quartz windows; 13: X-pinch; 14–17: Mach-Zehnder micro-interferometer; 18: focusing objective lens Sigma APO DG; 19: interference filter (532 nm); 20: Canon EOS 450D camera.

Two optical diagnostic techniques were used: shadow imaging and shearing interferometry. For shadow imaging, a CW laser (532 nm, ~ 100 mW) was used as a source of backlight, and a 4QuikE intensified camera was used for capturing the images with a frame time of 5 ns at different time delays τ_d with respect to the beginning of the discharge current. An objective lens (SIGMA APO DG) was used for imaging the area where the wires were crossing each other, providing a space resolution of ~ 40 μm . The Mach-Zehnder scheme was used for shearing interferometry, see Fig. 2. The mirrors had an aperture of $\sim 2.54 \times 10^{-2}$ m, and the beam-splitting cubes were $20 \times 20 \times 20$ mm³. The width of the field of visualization was $\sim 1.8 \times 10^{-2}$ m. A Nd:YAG laser (EXPLA NG301G, 532 nm, ~ 20 mJ, 6 ns) with a spectral width of the laser line of ~ 0.1 cm⁻¹ was used as a coherent source of illumination, and the same, i.e., SIGMA APO DG, objective lens was used for focusing the image of the wire intersection on the charge-coupled device of the Canon EOS 450D camera, providing a space resolution of ~ 10 μm .

III. EXPERIMENTAL RESULTS

A series of shadow and shearing interferogram images of an X-pinch in water (see Figs. 3–5) was recorded at different time delays τ_d . Similar to the experiments performed in vacuum, in the case of underwater X-pinchs, the generation of two jets lying along the acute angle bisectors was observed. In this case, however, the generation of these jets

can be described by a process of cumulation, similar to the effect of jet formation in a weakly compressible medium. The fast radial expansion of the wires begins at the location of the intersection of the wires. This leads to the generation of a quasi-spherical shock wave (SW). The front of this SW is interacting, but is not overlapping, with the fronts of cylindrical SWs, which are generated by the radial expansion of the wires. As a result, a region of a high pressure P_W is created behind the interacting fronts of these SWs [see Figs. 3 and 4 (in the plane of the wires, i.e., front view) and Fig. 5 (perpendicular to the plane of the wires, i.e., side view)].

At $\tau_d < 200$ ns, the generation of the jets can be determined by the dynamics of the highly pressurized metal plasma, and by its interaction with the self-magnetic fields of the discharge current. It is known from previous UEWE experiments⁸ that the strong density gradients realized at the SW front in water result in a strong scattering of the light of the backlighting laser. Therefore, the regions where high compression of water is realized are seen in various degrees of opaqueness. This phenomenon also explains why the SW fronts look dark on both shadow and shearing interferogram images. In the present experiments, until $\tau_d \leq 600$ ns the formation of the jets could not be observed, because the generated SWs during that time interval caused the backlight to be deflected in way that obscured the view of what lay behind the SW, including the expanding jets. Therefore, only at $\tau_d > 600$ ns does the region behind expanding SW front become transparent enough to allow the observation of the two oppositely directed jets. The time-of-flight dependence of these jets is shown in Fig. 6. These data show that, within the time interval of the observation, the velocity of jet propagation remains constant with the average value of $V_j \approx 2.5 \times 10^5$ cm/s.

IV. DISCUSSION

The experiments on underwater electrical explosion of X-pinch showed the formation of jets, propagating in opposite directions, with an average velocity of $V_j \approx 2.5 \times 10^5$ cm/s. Let us discuss the mechanism that can be responsible for this phenomenon. First, let us note that at $\tau_d > 200$ ns the discharge current and, respectively, the self-magnetic field have almost decayed, as well as the energy deposition into the exploding wires (at that time, the amplitude of the discharge current decreases to ≤ 7 kA). Thus, another explanation for the

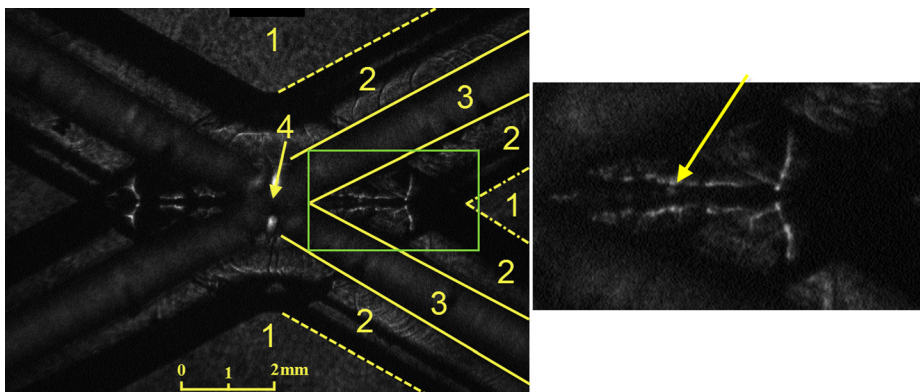


FIG. 3. Shadow image (left) obtained at $\tau_d \sim 900$ ns (front view). The shock wave fronts are marked by dashed lines and the exploding wires are outlined by solid lines. The smaller image on the right is zoom on the section of the shadow image confined by the rectangle. The copper jet is clearly seen (marked by the arrow). Numeric markings: (1) Undisturbed water; (2) Compressed water behind the shock wave front. (3) Exploding wire. (4) “Hot spot” (marked by the arrow).

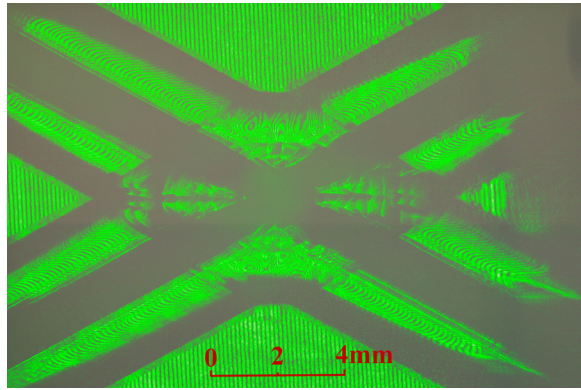


FIG. 4. Shearing interferogram obtained at $\tau_d \sim 900$ ns (front view).

emergence of the jets, other than acceleration by the magnetic pressure, is needed.

The pressure P_W behind the front of the cylindrical SW can be estimated using the SW velocity. The latter was obtained by the time-of-flight data of the expansion of this SW near the point of the intersection of the wires (see Fig. 7). The resulting average velocity of the SW is $D_{SW} = 2.27 \times 10^3$ m/s. By using the polytropic equation-of-state (EOS) of water,¹⁰ one can estimate the pressure behind the front of this SW as $P_W \approx 9 \times 10^8$ Pa, the density as $\sim 1.2\rho_0$, and the sound velocity as $c_W \approx 1.8c_0$, where $\rho_0 = 10^3$ kg/m³ and $c_0 \approx 1.5 \times 10^3$ m/s are the density and speed of sound in undisturbed water, respectively.

Let us make an estimation of the parameters of the expanding wire at $\tau_d \sim 900$ ns, i.e., the averaged density, temperature, and radial velocity (see Fig. 3). The density of the copper can be estimated as $\rho_{Cu} \approx \rho_{Cu0} (d_0/d)^2$, where $d_0 = 10^{-4}$ m is the initial diameter of the wire and $\rho_{Cu0} \approx 9 \times 10^3$ kg/m³ is the normal density of copper. At that time, i.e., $\tau_d \sim 900$ ns, the diameter of the expanding wire is $d \approx 10^{-3}$ m, and, therefore, the density of the copper is $\rho_{Cu} \approx 10^2$ kg/m³, which results in a density of the copper atoms of $n_{Cu} \approx 5.6 \times 10^{26}$ m⁻³. The radial expansion velocity of the exploding wire can be calculated using the experimentally obtained temporal dependence of the wire radius,

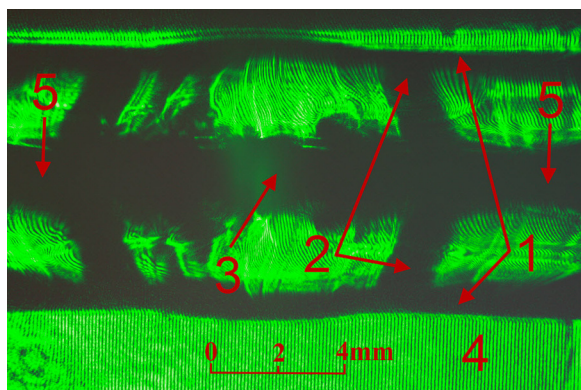


FIG. 5. Shearing interferogram obtained perpendicular to the X-pinch plane (side view) in the vicinity of the intersection of the wires. The time delay is $\tau_d \approx 1 \mu$ s. (1) Shockwave fronts. (2) Interacting shockwave fronts. (3) Point of the intersection of the wires (“hot spot”). (4) Undisturbed water (5) Plasma channels (radially expanding wire material).

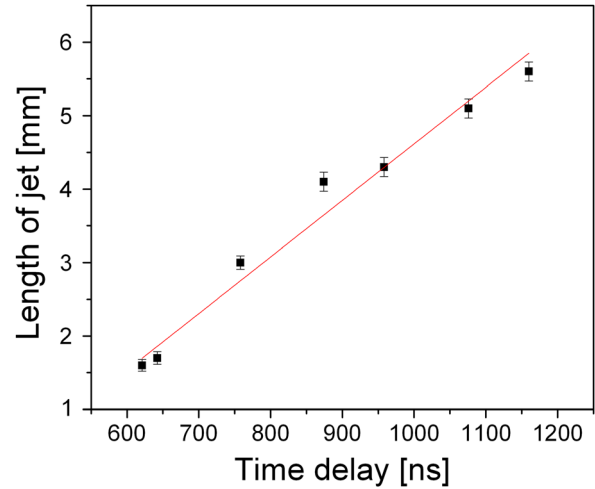


FIG. 6. Temporal dependence of the length of the cumulative jets.

which is shown in Fig. 7. One can see that the radial expansion of the wire is significantly slower than the SW radial expansion, which is almost constant. The latter is a rather surprising result. Indeed, in order to keep the SW velocity constant, the energy should be continuously deposited into the exploding wire, which acts as a cylindrical piston. However, the energy deposition into the wire has almost terminated at $\tau_d \geq 200$ ns (see Fig. 1). In this case, the trajectory of the SW at $\tau_d \geq 200$ ns (see solid line in Fig. 7), simulated by the Witham model,¹¹ shows a radial velocity of the SW that is significantly slower than the measured constant velocity of the SW. Thus, in order to explain the constant velocity of the SW expansion, one has to assume the existence of an additional energy flux, which is delivered to the layer of water between the front of the SW and the boundary of the expanding wire, after the energy deposition into the wires has been terminated. One can assume that the appropriate source of this energy flux can be the quasi-spherically expanding SW, originating from the plasma spot formed at the location of the intersection of the wires, due to temperature and density gradients existing in this location. This expanding “hot spot”

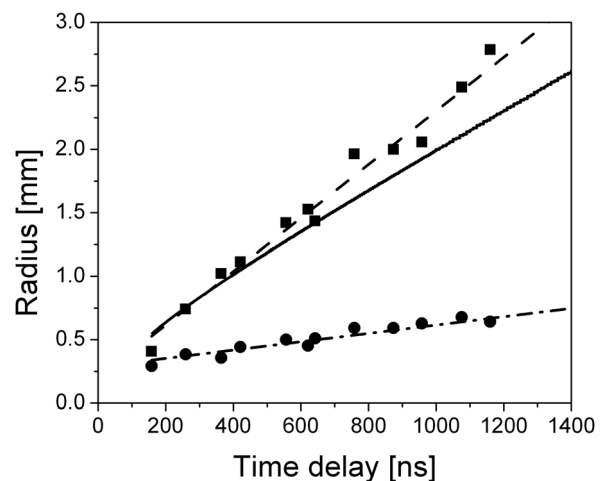


FIG. 7. Temporal dependencies of the radii of the expanding plasma channel (circles) and of the cylindrical SW (squares). The solid line is the simulated trajectory of the SW, following Witham’s approach.¹¹

generates hydrodynamic flows along the cylindrical channels formed between the expanding boundaries of wires and the SWs front. These additional hydrodynamic flows keep the velocity of the SWs almost constant. In this case, the pressure at the boundary of the expanding wire should be approximately equal to the pressure behind the SW front, i.e., $P_{Cu} \approx P_W \approx 9 \times 10^8$ Pa. At $\tau_d \sim 900$ ns, the density of atoms in the expanding wire decreases by $\sim 10^2$ times, which allows one to estimate the sound velocity roughly as $c_{Cu} = \sqrt{\gamma P_{Cu} / \rho_{Cu}} \approx 4 \times 10^3$ m/s. This value of the sound velocity is significantly larger than the expansion velocities of the wire ($V_0 \approx 6 \times 10^2$ m/s). The latter allows the collision of the two expanding wires to be considered as the collision of two weakly compressible flows.

Now, let us apply the model of cumulation based on the collision of two planar slabs¹² generating a pair of oppositely directed planar jets. This model considers the collision of two identical flat slabs with tangent velocities V_0 at angle α . In the laboratory coordinate system, one obtains that a fast and a slow jet are generated co-moving along the bisector of the angle α , the fast one with a velocity $V_{Fj} = V_0 \text{ctg}(\alpha/4)$ and the slow one with a velocity $V_{Sj} = V_0 \text{tg}(\alpha/4)$. The total mass of the ejected material, $m_0 = m_1 + m_2$, is divided between the fast (m_1) and the slow jet (m_2). This model also predicts the ratio between these masses, $(m_1/m_2) = \text{tg}^2(\alpha/4)$, and the ratio between their cross-sections, $(S_1/S_2) = (m_1/m_2)$. The fast jet has a much smaller cross-section, but it carries the main part of the kinetic energy of the colliding slabs. In order to explain these cumulative jets, this theory assumes an infinite width of the slabs, so that the expansion of the material at the edges of these slabs will not influence the location of the slabs' collision. In the case of a collision of two cylinders in a similar configuration, this theory is invalid. In the present experiment, however, the collision of two cylindrically expanding wires produces the jets that are similar to those produced in the case of colliding flat slabs. Indeed, the expansion of these wires is limited by the pressure of the surrounding water in the direction perpendicular to the direction of propagation of the jets. By taking the experimental values of the angle between the wires $\alpha \approx 58^\circ$ and of the velocity of the cylindrical SWs $V_0 \approx 6 \times 10^2$ m/s, one obtains the value of the velocity of the fast jet of $V_{Fj} \approx 2.34 \times 10^3$ m/s, which agrees satisfactory well with the experimentally obtained value of the velocity of the jets, $V_j \approx 2.5 \times 10^3$ m/s.

V. CONCLUSION

In conclusion, the collision of the exploding wires generated by underwater electrical explosion in the X-pinch configuration creates fast-moving cumulative jets similar to those generated by the collision of metal slabs, accelerated by the chemical explosion. The properties of these jets are determined by the parameters of the electrical explosion and their interaction with the water, compressed by the SW generated by the exploded wires. This method of generation of cumulative jets and their interaction with low-compressible media is significantly simpler than common methods, and allows the application of optical diagnostics for the observation of the dynamics of the jets.

ACKNOWLEDGMENTS

This research was supported by the Center for absorption in Science, Ministry of Immigrant Absorption, State of Israel and Israeli Science Foundation grant #99/12.

- ¹G. V. Ivanenko, S. A. Pikuz, D. A. Sinars, V. Stepnievski, D. A. Hammer, and T. A. Shelkovenko, *Plasma Phys. Rep.* **26**, 868 (2000).
- ²D. B. Sinars, S. A. Pikuz, T. A. Shelkovenko, K. M. Chandler, and D. A. Hammer, *Rev. Sci. Instrum.* **72**, 2948 (2001) and references therein.
- ³J. S. Green, S. N. Bland, M. Collett, A. E. Dangor, K. Krushelnik, F. N. Beg, and I. Ross, *Appl. Phys. Lett.* **88**, 261501 (2006).
- ⁴F. N. Beg, R. B. Stephens, H.-W. Xu, D. Haas, S. Eddinger, G. Tynan, E. Shipton, B. DeBono, and K. Wagshal, *Appl. Phys. Lett.* **89**, 101502 (2006).
- ⁵P. F. Knapp, S. A. Pikuz, T. A. Shelkovenko, D. A. Hammer, and S. B. Hansen, *Rev. Sci. Instrum.* **82**, 063501 (2011) and references therein.
- ⁶D. M. Haas, S. C. Bott, J. Kim, D. A. Mariscal, R. E. Madden, Y. Eshaq, U. Ueda, G. Collins, K. Gunasekera, F. N. Beg, J. P. Chittenden, N. Niasse, and C. A. Jennings, *Astrophys. Space Sci.* **336**, 33 (2011).
- ⁷S. M. Zakharov, G. V. Ivanenkov, A. A. Kolomenskii, S. A. Pikuz, A. I. Samokhin, and I. Ulshmid, *Sov. Tech. Phys. Lett.* **8**, 456 (1982).
- ⁸Ya. E. Krasik, A. Fedotov, D. Sheftman, S. Efimov, A. Sayapin, V. Tz. Gurovich, D. Veksler, G. Bazalitski, S. Gleizer, A. Grinenko, and V. I. Oreshkin, *Plasma Sources Sci. Technol.* **19**, 034020 (2010) and references therein.
- ⁹I. V. Sokolov, *Sov. Phys. Usp.* **33**, 960 (1990).
- ¹⁰Ya. B. Zel'dovich and Yu. P. Raizer, *Physics of Shock Waves and High-Temperature Hydrodynamic Phenomena* (Academic Press, NY, 1966).
- ¹¹G. B. Whitham, *Linear and Nonlinear Waves* (John Wiley & Sons, Inc., New York, 1974).
- ¹²F. A. Baum, K. P. Stanyukovich, and B. I. Shekhter, *Physics of an Explosion* (Army Engineer Research and Development Labs, Fort Belvoir, VA 1959).